Review of Scientific Instruments

Denoising of surface electromyogram based on complementary ensemble empirical mode decomposition and improved interval thresholding

Cite as: Rev. Sci. Instrum. **90**, 035003 (2019); https://doi.org/10.1063/1.5057725
Submitted: 15 September 2018 . Accepted: 05 March 2019 . Published Online: 22 March 2019

Xugang Xi, Yan Zhang, Yunbo Zhao, Qingshan She, and Zhizeng Luo

View Online Export Citation CrossMark



© 2019 Author(s).

Review of Scientific Instruments ARTICLE scitation.org/journal/rsi

Denoising of surface electromyogram based on complementary ensemble empirical mode decomposition and improved interval thresholding

Cite as: Rev. Sci. Instrum. 90, 035003 (2019); doi: 10.1063/1.5057725
Submitted: 15 September 2018 • Accepted: 5 March 2019 •
Published Online: 22 March 2019

View Online Export Citation CrossMark

Xugang Xi,[1,a)] Yan Zhang,[1] Yunbo Zhao,[2,a)] Qingshan She,[1] and Zhizeng Luo[1]

AFFILIATIONS

[1]School of Automation, Hangzhou Dianzi University, Hangzhou 310018, China
[2]College of Information Engineering, Zhejiang University of Technology, Hangzhou 310023, China

[a)]**Authors to whom correspondence should be addressed:** xixi@hdu.edu.cn and ybzhao@ieee.org

ABSTRACT

Surface electromyogram (sEMG) signals are physiological signals that are widely applied in certain fields. However, sEMG signals are frequently corrupted by noise, which can lead to catastrophic consequences. A novel scheme based on complementary ensemble empirical mode decomposition (CEEMD), improved interval thresholding (IT), and component correlation analysis is developed in this study to reduce noise contamination. To solve the problem of losing desired information from sEMG, an sEMG signal is first decomposed using CEEMD to obtain intrinsic mode functions (IMFs). Subsequently, IMFs are selected via component correlation analysis, which is a measure used to select relevant modes. Thus, each selected IMF is modified through improved IT. Finally, the sEMG signal is reconstructed using the processed and residual IMFs. Root-mean-square error (RMSE) and signal-to-noise ratio (SNR) are introduced as evaluation criteria for the sEMG signal from the standard database. With SNR varying from 1 dB to 25 dB, the proposed method increases SNR by at least 1 dB and reduces RMSE compared with stationary wavelet transform and other denoising algorithms based on empirical mode decomposition. Moreover, the proposed method is applied to hand motion recognition. Results show that the rate of the denoised sEMG signal is higher than that of the raw sEMG signal.

Published under license by AIP Publishing. https://doi.org/10.1063/1.5057725

I. INTRODUCTION

Surface electromyogram (sEMG) is a technique used to generate bioelectric signals that can reflect information related to muscle and body behavior.[1] sEMG signals are extensively used in various fields, such as sports medicine, rehabilitation training, and mechanical control.[2–4] In addition, sEMG signals are extremely weak, with magnitudes limited within the μV range. Moreover, sEMG signals are nonlinear, nonstationary, and distributed between 10 Hz and 500 Hz. However, these signals are vulnerable to corruption by noises due to their characteristics. Three types of noise occur: power line interference, white Gaussian noise, and baseline wandering.[5] Therefore, denoising sEMG signals is a prerequisite[6] for analyzing and applying sEMG information.

Previous studies have shown that the wavelet threshold denoising algorithm can be used to reduce noise in sEMG.[4] Wavelet transform exhibits good local properties in the time and frequency domains. However, the wavelet base and the number of decomposition layers should be selected by an expert. Research shows that wavelet bases and decomposition layers exert considerable influences on the denoising result.[7] To overcome the aforementioned drawbacks, wave atom transform has been proposed to replace wavelet transform.[8] Wave atom transform is a novel multiscale decomposition method for analyzing signals corrupted by noise and uncertainty.[9]

The empirical mode decomposition (EMD) algorithm is used in denoising signals by overcoming the shortcomings of wavelet denoising.[10–15] EMD can decompose a nonstationary signal into

intrinsic mode functions (IMFs), which present different time scales of the original signal.[16] Wu and Huang[17] proposed ensemble EMD (EEMD) because mode mixing in EEMD is a data-driven analysis algorithm that adds white noise to a noisy signal before the signal is decomposed. Simultaneously, EEMD considers noise contamination induced by residue. To resolve the aforementioned problem, Yeh *et al.*[18] proposed a new noise-assisted analysis method, namely, complementary EEMD (CEEMD), in which white noises are added with a pair of opposite noises to the target signal. Experiments show that the improved method is better than the general denoising method and its application is convenient and flexible.[19] Inspired by wavelet thresholding, Kopsinis and Mclanglin[20] developed a novel EMD interval thresholding (IT) (i.e., EMD-IT) denoising method, and various signals were used to test this algorithm. In their method, a zero-crossing interval is regarded as a unit that presents thresholding performance. In this manner, the approach can overcome discontinuity.[21,22]

The effective selection of relevant modes is a critical problem in EMD-based denoising methods.[23] Yang[24] proposed a new criterion, namely, similarity measure, for selecting relevant modes. However, similarity measure should be fitted to analyze stationary signals. Chen[25] developed a correlation analysis algorithm for selecting representative modes for fault diagnosis. Inspired by the correlation analysis algorithm, we used component correlation analysis to select the most representative modes as relevant modes. In the current study, a novel method based on CEEMD, component correlation analysis, and improved IT was proposed to eliminate noise contamination in sEMG signals. To reduce the loss of desired information from sEMG, CEEMD was used to decompose raw signals into IMFs. Then, component correlation analysis was applied to calculate the correlation coefficients between the raw sEMG signals and each IMF to select relevant modes. Subsequently, the IMFs with large correlation coefficients were processed via improved IT. Finally, the signal was reconstructed using the processed IMFs and the unprocessed residual IMFs. For sEMG from the standard database, the proposed method achieved better denoising performance compared with those of EMD and EMD-IT. Previous experiments showed that noise-free signals would increase a system's recognition rate.[26–28] In this regard, an application experiment on denoised sEMG signal was conducted to evaluate the performance of the proposed method.

The remainder of this paper is organized as follows: Sec. II presents the proposed method and reviews the basic theories of related algorithms. Section III conducts a case study to evaluate the proposed approach. Section IV applies the proposed method to an sEMG signal denoising experiment for motion recognition. Section V discusses and concludes the study.

II. METHODS

We propose a novel sEMG denoising method based on CEEMD, component correlation analysis, and improved IT. The flow diagram of the proposed approach is shown in Fig. 1, and the steps are as follows:

(1) The raw sEMG signal is decomposed via CEEMD.
(2) The correlation coefficients of each IMF and the original signal are calculated. Appropriate IMFs are selected using component correlation analysis.

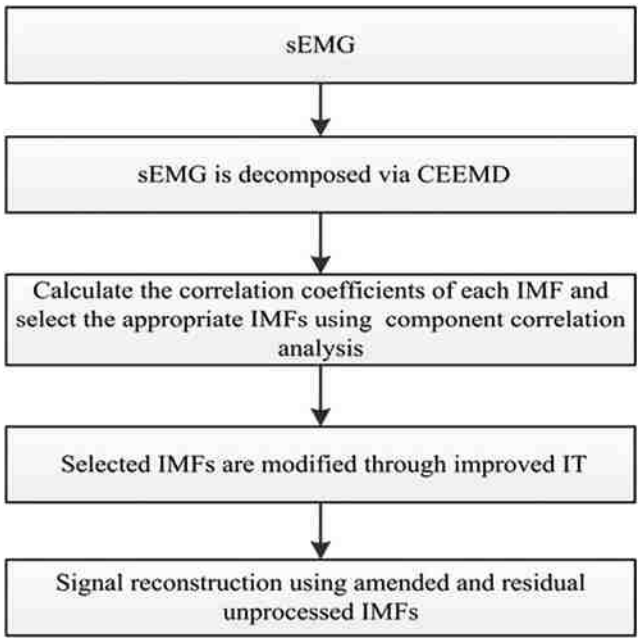

FIG. 1. Framework of the proposed method.

(3) The selected IMFs are modified through improved IT.
(4) sEMG is reconstructed using the modified and unprocessed residual IMFs.

A. CEEMD

CEEMD is an improved method based on the EMD algorithm proposed by Huang.[16] EMD decomposes signals into IMFs, where each IMF denotes a dynamic feature. An IMF must meet two requirements. (1) The numbers of maximum points and zero crossings (ZCs) for a time series should be equal to or different by a maximum of one. (2) The average of the upper and lower envelopes should be zero at any moment. Following the standard principle of EMD, an sEMG signal $x(t)$ is decomposed as follows:

$$x(t) = \sum_{i=1}^{n} imf_i(t) + r_n(t), \tag{1}$$

where $imf_i(t)$ is the ith IMF and $r_n(t)$ is a RES that presents the trend of a signal.

If $r_n(t)$ is regarded as the $(n+1)th$ IMF, then Eq. (1) can be rewritten as follows:

$$x(t) = \sum_{i=1}^{N} C_i(t), \tag{2}$$

where $C_i(t)$ is the ith IMF and $N = n+1$.

In EEMD, white noise is added to the original signal to overcome mode mixing.[17] In CEEMD, white noises are added in pairs. Han and Mirko[29] verified the advantages of CEEMD. For sEMG $x(t)$, the CEEMD algorithm includes the following steps:

(1) In CEEMD, pairs of white noises, which consist of a positive noise and a negative noise, are added to the original data to

Published under license by AIP Publishing

generate two sets of ensemble IMFs

$$\begin{bmatrix} x_j^+(t) \\ x_j^-(t) \end{bmatrix} = \begin{bmatrix} 1 & 1 \\ 1 & -1 \end{bmatrix} \begin{bmatrix} x(t) \\ N_j(t) \end{bmatrix}, \quad j = 1, 2, \ldots, M, \tag{3}$$

where $x(t)$ denotes the original data, $N_j(t)$ is the added white noise, x_j^+ is the sum of the original data with positive noise, x_j^- is the sum of the original data with negative noise, and M is the number of trials.

(2) $x_j^+(t)$ and $x_j^-(t)$ are decomposed to obtain the ith IMF components $C_{ij}^+(t)$ and $C_{ij}^-(t)$ using EMD.

(3) The decomposition result, i.e., the ith IMF $C_i(t)$, is obtained by averaging multiple components as follows:

$$C_i(t) = \frac{1}{2M} \sum_{j=1}^{M} (C_{ij}^+(t) + C_{ij}^-(t)). \tag{4}$$

Then, the signals decomposed with positive and negative noises will take positive and negative residues, respectively. Errors can be reduced based on the influence of the positive and negative residues.

B. Component correlation analysis

Component correlation analysis is used to examine the correlation between the original sEMG and IMFs. The IMFs with larger correlation coefficients than the reference correlation coefficient are selected. The correlation coefficient between sEMG $x(t)$ and each component IMF $C_i(t)$ is calculated as follows:

(1) The covariance between $x(t)$ and $C_i(t)$ is calculated

$$\begin{aligned} c_{xC}(i) &= E\{[x(t) - u_x][C_i(t) - u_{Ci}]\} \\ &= \lim_{T\to\infty} \frac{1}{T} \int_0^T \{[x(t) - u_x][C_i(t) - u_{Ci}]\} dt, \end{aligned} \tag{5}$$

where $c_{xC}(i)$ represents the covariance of $x(t)$ and $C_i(t)$, u_x denotes the mean values of $x(t)$, and u_{Ci} indicates the mean values of $C_i(t)$.

(2) The correlation coefficient is calculated

$$\rho_{xC}(i) = \frac{c_{xC}(i)}{\sigma_x \sigma_{Ci}}, \tag{6}$$

where $\rho_{xC}(i)$ represents the correlation between $x(t)$ and $C_i(t)$ and σ_x and σ_{Ci} are the standard variances of $x(t)$ and $C_i(t)$, respectively.

(3) The reference correlation coefficient T is calculated.

The thresholding T can filter IMFs with small correlation coefficients. The thresholding T can be calculated as follows:

$$T = \frac{1}{N} \sum_{i=1}^{N} \rho_{xC}(i). \tag{7}$$

N is the number of IMFs. The ith IMF is selected when $\rho_{xC}(i) > T$.

C. Improved IT

The wavelet thresholding denoising algorithm is effective in denoising noise in sEMG signals. The wavelet coefficients are modified when they are lower than the thresholding value. Stationary wavelet transform (SWT)-based denoising has been proven to derive good sEMG signals.[30] Wavelet thresholding can be applied directly to EMD, but EMD direct thresholding (EMD-DT), whether hard or soft, can have catastrophic consequences.[24]

IT is proposed to overcome the discontinuity of direct thresholding. We regard the samples from adjacent zero-crossing intervals as mode cells. In the interval $Z_i^{(j)} = [z_i^{(j)} z_i^{(j+1)}]$ j = 1, 2, . . ., N_i; N_i is the sum zero-crossing number of the ith IMF, and $z_i^{(j)}$ is the jth adjacent zero-crossing of the ith IMF. Hence, the method is translated into[20]

$$\tilde{C}_i(Z_i^{(j)}) = \begin{cases} C_i(Z_i^{(j)}) & \left|C_i(r_i^{(j)})\right| > T_i \\ 0 & \left|C_i(r_i^{(j)})\right| \le T \end{cases} \tag{8}$$

and

$$\tilde{C}_i(Z_i^{(j)}) = \begin{cases} C_i(Z_i^{(j)}) \frac{\left|C_i(r_i^{(j)})\right| - T_i}{\left|C_i(r_i^{(j)})\right|} & \left|C_i(r_i^{(j)})\right| > T_i \\ 0 & \left|C_i(r_i^{(j)})\right| \le T \end{cases} \tag{9}$$

for hard and soft thresholding, respectively. In the preceding formulas, $C_i(r_i^{(j)})$ represents the single extreme of the adjacent zero-crossing interval $Z_i^{(j)}$, $C_i(Z_i^{(j)})$ denotes the sample amplitude from zero-crossing intervals $Z_i^{(j)}$ to $Z_i^{(j+1)}$, and $\tilde{C}_i(Z_i^{(j)})$ is the thresholded version of the ith IMF.

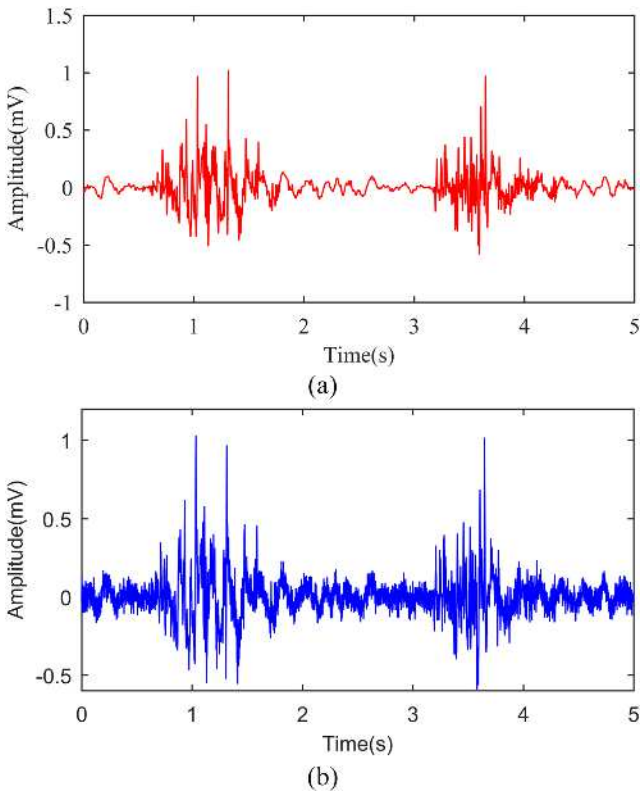

FIG. 2. (a) Clean sEMG signals (denoted as sEMG1) collected from the standard database. (b) Noisy sEMG signals.

Published under license by AIP Publishing

A considerable difference exists between noise-only and noisy IMFs. The energy of IMF exhibits linear reduction in a semilog diagram.[20] The energy of noise-only IMF can be calculated as follows:

$$\hat{E}_i = \frac{E_1^2}{\beta}\rho^{-k}, \mathrm{k} = 2, 3, 4, \ldots, \tag{10}$$

where E_1^2 denotes the energy of the first IMF and the values of parameters β and ρ are set as 0.719 and 2.01, respectively.

Each IMF is corrupted by noise, thereby indicating that noise has a different energy in each IMF.[20] Hence, thresholding is dependent on scaling and is a multiple of the universal thresholding of IMFs

$$T_i = C\sqrt{\hat{E}_i 2\ln N}, \tag{11}$$

where C is a constant parameter. The best C for CEEMD is 0.6–0.8. C is 0.8–0.9 for translation invariant thresholding,[20] as confirmed by our experiments. After the analysis, we set C as 0.8.

The application of hard IT can have catastrophic consequences due to the discontinuity at the instant when $\left|C_i(r_i^{(j)})\right| = T_i$. Certain effects cause the filtered reconstructed signal to oscillate randomly at the thresholding, which deteriorates the smoothness of the reconstructed signal. In contrast with hard IT, soft IT can reduce the effects of discontinuity. However, the constant deviation will decrease the signal-to-noise ratio (SNR) and increase the root-mean-square error (RMSE), thereby resulting in poor denoising performance.

The new threshold function established in this study can effectively compensate for the limitations of the hard and soft thresholding methods, which is defined as follows:

$$\tilde{C}_i\left(Z_j^{(i)}\right) = \begin{cases} C_i(Z_i^{(j)})\left(1 - \left(\frac{T_i}{\left|C_i(r_i^{(j)})\right|}\right)^n\right) & \left|C_i(r_i^{(j)})\right| > T_i \\ 0 & \left|C_i(r_i^{(j)})\right| \le T_i \end{cases}, \tag{12}$$

where n is a tunable parameter. $Z_i^{(j)}$ denotes the data of adjacent zero-crossing intervals. When n is close to infinity, the improved IT is approximately hard IT. Similarly, the improved IT is soft IT when n is set as 1. The function curve smoothens with a decrease in n. When the noisy signal contains numerous saltation points, the improved IT should be close to hard IT. Similarly, when the noisy signal is smooth, the improved IT should be close to soft IT. That is, the improved IT can exhibit the advantages of hard and soft IT. When an IMF represents a high-frequency component, a large n is set to process this IMF.

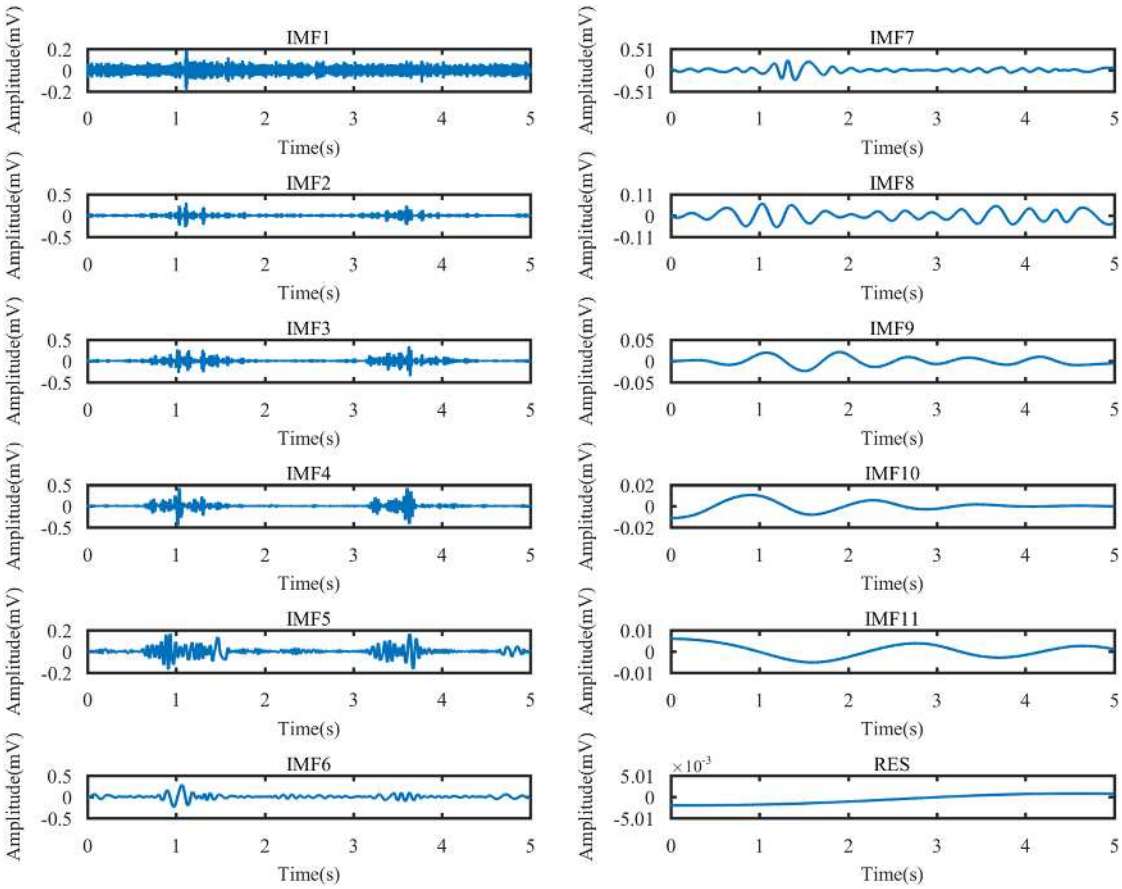

FIG. 3. Eleven IMFs and RES decomposed via CEEMD.

Published under license by AIP Publishing

TABLE I. Correlation coefficients between the original signal and each IMF.

IMF component	Correlation coefficient	IMF component	Correlation coefficient
IMF1	0.1749	IMF7	0.4183
IMF2	0.3550	IMF8	0.1675
IMF3	0.4172	IMF9	0.1160
IMF4	0.4681	IMF10	0.0017
IMF5	0.3602	IMF11	−0.0041
IMF6	0.4587	RES	0.0012
T	0.2161		

D. Reconstruction of sEMG signal

The modified IMF is defined as $\tilde{C}_i$, and the residual IMF is C_i, where i is the order of IMFs. Hence, the sEMG signal $\tilde{x}(t)$ is reconstructed as follows:

$$\tilde{x}(t) = \sum_{q=1}^{m} \tilde{C}_i(q) + \sum_{p=1}^{N-1-m} C_i(p), \tag{13}$$

where q is the number of modified IMFs and p is the number of IMFs. In residual IMFs with minimal noise energy,[20] the first component, IMF1, is abandoned because the proportion of noise in IMF1 is considerable.[18]

III. EXPERIMENT RESULTS

The clean signals (denoted as sEMG1 and sEMG2) were derived from the standard database with a sampling rate of 1000 Hz. White Gaussian noise was added to obtain a noisy sEMG signal. Figure 2 shows the clean and noisy sEMG (denoted as sEMG1) signals with 15 dB SNR.

A noisy sEMG signal $x(t)$ is set as

$$x(t) = s(t) + \delta n(t), \tag{14}$$

where $s(t)$ denotes the clean sEMG signal from the standard database, $n(t)$ indicates white Gaussian noise, and δ represents the scale factor of noise. The artificially noisy sEMG signals are quantified using the SNR levels, which vary from 1 dB to 25 dB to verify the performance of the proposed method.

The noisy signal (denoted as sEMG1) was decomposed via CEEMD. Figure 3 presents the result of 11 IMFs and RES.

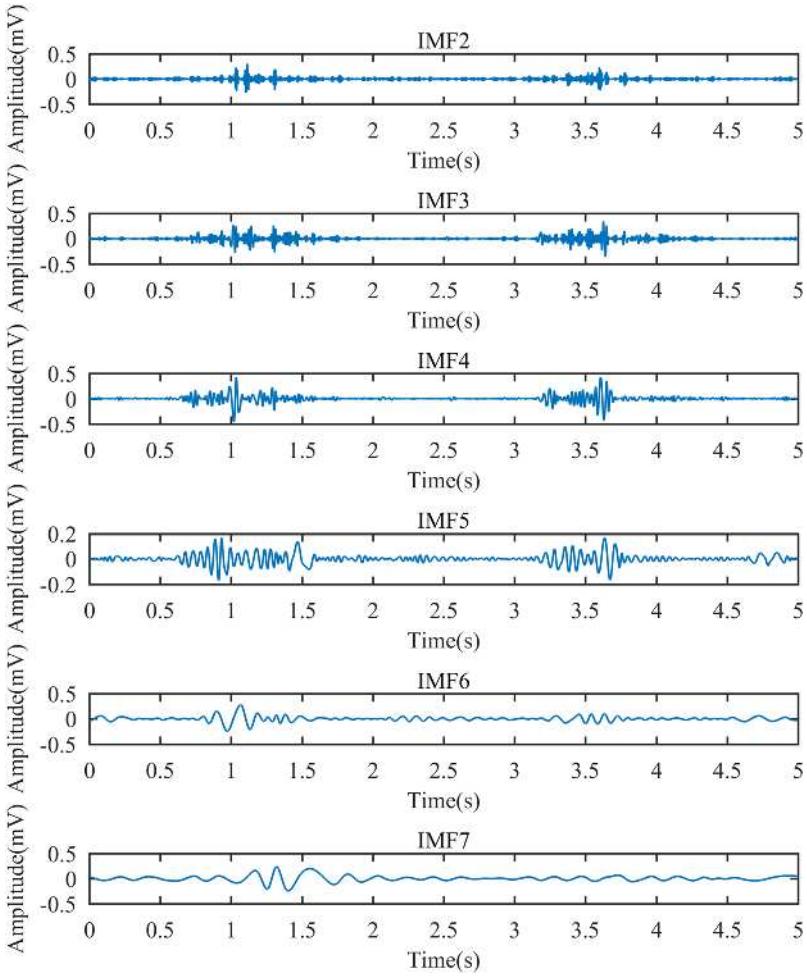

FIG. 4. IMFs denoised through improved IT.

Published under license by AIP Publishing

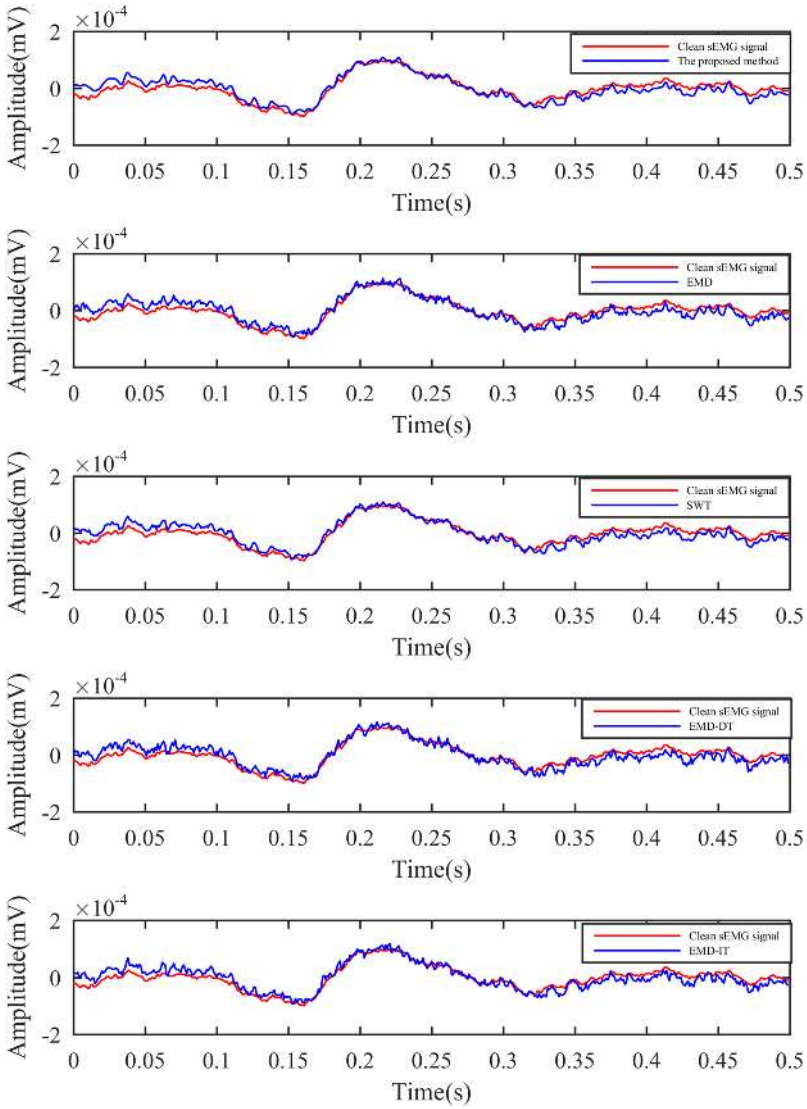

FIG. 5. Reconstructed and clean sEMG signals using different methods.

To further illustrate the selected IMFs, we obtained the thresholding using Eq. (7), where T = 0.2161. Table I reports the correlation coefficients between the noisy signal $x(t)$ and each IMF. The coefficients of IMFs 2, 3, 4, 5, 6, and 7 are higher than T. In addition, IMFs 2, 3, 4, 5, 6, and 7 are processed via improved IT. The results are presented in Fig. 4.

We used the EMD and EMD-IT methods in comparison with the proposed method. RMSE and SNR were introduced as evaluation

TABLE II. Comparison of the SNR_{out} and RMSE of the denoised sEMG signal (sEMG1).

SNR_{in}	EMD [SNR_{out} (dB)/RMSE]	SWT [SNR_{out} (dB)/RMSE]	EMD-DT [SNR_{out} (dB)/RMSE]	EMD-IT [SNR_{out} (dB)/RMSE]	Proposed method [SNR_{out} (dB)/RMSE]
1 dB	3.613/**0.0535**	4.276/0.0656	3.765/0.0762	3.988/0.0802	**5.246**/0.0746
5 dB	7.647/0.0265	7.895/0.0401	8.995/**0.0356**	8.237/0.0574	**9.633**/0.0452
10 dB	12.858/0.0095	13.062/**0.0082**	12.965/0.0090	13.022/0.0094	**14.321**/0.0086
15 dB	15.888/0.0067	**17.736**/0.0045	15.865/0.0070	17.423/0.0056	17.632/**0.0043**
20 dB	21.231/0.0045	22.450/0.0034	22.235/0.0034	22.356/0.0032	**25.124**/**0.0023**
25 dB	28.781/0.0015	27.456/0.0020	26.332/0.0019	24.542/0.0025	**28.795**/**0.0013**

Published under license by AIP Publishing

TABLE III. Comparison of the SNR_{out} and RMSE of the denoised sEMG signal (sEMG2).

SNR_{in}	EMD (SNR_{out} (dB)/RMSE)	SWT (SNR_{out} (dB)/RMSE)	EMD-DT (SNR_{out} (dB)/RMSE)	EMD-IT (SNR_{out} (dB)/RMSE)	Proposed method (SNR_{out} (dB)/RMSE)
1 dB	3.864/0.0965	4.776/0.0885	4.765/0.0762	4.986/0.0802	**5.793/0.0696**
5 dB	7.421/0.0485	8.595/0.0311	8.395/0.0405	8.456/0.0373	**9.986/0.0253**
10 dB	12.967/0.0125	13.523/0.0113	13.786/0.0103	14.076/0.0099	**15.541/0.0089**
15 dB	17.097/0.0079	17.536/**0.0060**	16.385/0.0077	17.876/0.0065	**18.976**/0.0061
20 dB	22.576/0.0043	**24.750**/0.0023	23.565/0.0037	24.055/0.0029	24.542/**0.0021**
25 dB	25.567/0.0012	25.996/0.0011	25.372/0.0015	**27.042**/0.0011	26.005/**0.0009**

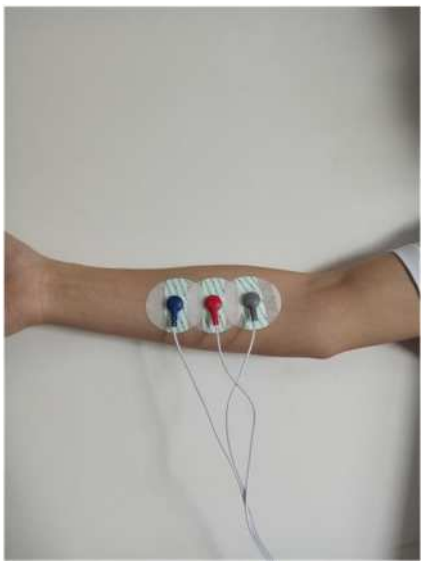

FIG. 6. sEMG sensor placement.

criteria

$$RMSE = \sqrt{\frac{1}{n}\sum_{i=1}^{N}(x-\tilde{x})^2}, \tag{15}$$

$$SNR = 10lg\left(\sum_{i=1}^{N}x^2 / \sum_{i=1}^{N}(x-\tilde{x})^2\right), \tag{16}$$

where x is the sEMG signal and $\tilde{x}$ represents the denoised sEMG signal.

We used modified IMFs 2, 3, 4, 5, 6, and 7; the residual IMFs 8, 9, 10, and 11; and RES to reconstruct the sEMG signal using Eq. (13). Figure 5 presents the reconstructed sEMG and clean signals using different methods.

Tables II and III provide the denoising performance of the five methods with SNR_{in} varying from 1 dB to 25 dB. The data before the brackets pertain to SNR_{out}, whereas the remaining data denote RMSE. The denoising performance of all the methods remains stable throughout an increase in SNR_{in}. However, the closer SNR_{in} is to 25 dB, the worse the denoising performance of the EMD method. By contrast, the proposed method provides the best result compared with the other methods in nearly all the cases. Moreover, the RMSE of the proposed method is less than those of the other methods.

IV. APPLICATION EXPERIMENT OF sEMG SIGNAL DENOISING TO MOTION RECOGNITION

We verified the sEMG denoising method for motion recognition. The two sEMG channels were recorded from the flexor palmar and long palmar using a self-constructed signal acquisition system with a sampling frequency of 1000 Hz. As shown in Fig. 8, four motions of the upper limb, namely, hand open, hand close, wrist flexion, and wrist extension, were selected (Figs. 6 and 7).

Five features were extracted, namely, the integral of variance (VAR), Wilson amplitude (WAMP), zero crossing (ZC), mean frequency (MF), and energy of wavelet coefficient (EWT).[30] The Gaussian kernel support vector machine (GK-SVM) was selected for classification.[31]

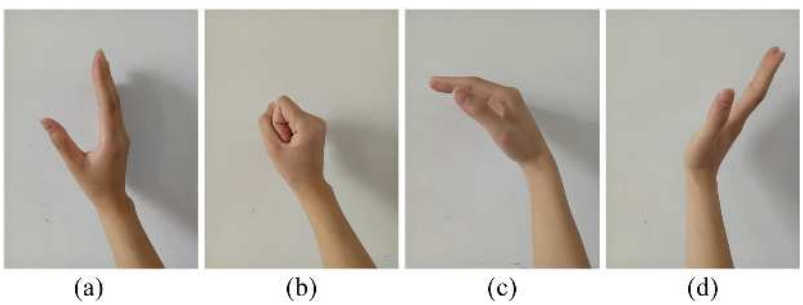

FIG. 7. Four hand motions: (a) Hand open, (b) hand close, (c) wrist flexion, and (d) wrist extension.

Published under license by AIP Publishing

TABLE IV. Recognition rates of raw and denoised sEMG signals (%).

Motions	Raw sEMG	Denoised sEMG
Hand open	77.5	87.8
Hand close	76.2	85.6
Wrist flexion	78.5	87.9
Wrist extension	80.1	90.4
Average	78.1	87.9

The recognition results are presented in Table V. We observe that the direct application of raw sEMG has a negative effect. By contrast, the proposed method exhibits better performance in all the motions, particularly wrist extension. Moreover, the average accuracy rate of motion recognition was improved from 78.5% to 87.9% compared with the raw sEMG. The proposed method achieves better performance based on the aforementioned denoising result because it diminishes the noise component.[32]

V. DISCUSSIONS AND CONCLUSION

A CEEMD-based improved IT framework for denoising sEMG signals was presented and evaluated experimentally.

As an extension of EMD, CEEMD adaptively separates nonlinear and nonstationary signals into several IMFs, which can represent different dynamic properties from various oscillation levels. CEEMD not only produces several more strictly band-restricted IMFs compared with EMD but also reduces the computational complexity of EEMD. Given that noise has different dynamic properties from useful components, noise can be removed easily from special band-restricted IMFs. To optimize the CEEMD-based framework, improved IT, which could adapt thresholding to specific IMFs, was proposed.

As shown in Fig. 5, the proposed method retains more useful information compared with the other methods. Furthermore, the comparison results of five different methods are presented in Tables II and III. Notably, the proposed method achieved better denoising performance at nearly all SNR levels. Evidently, the noise level influences the efficiency of the denoising methods. When SNR is high, the performance of the proposed method is unsatisfactory because noise distribution is dispersed in IMFs and the thresholding procedure is limited. To evaluate the denoising performance of the proposed method, we applied the method to motion recognition. The proposed method can considerably enhance recognition rates, as shown in Table IV. The analysis result can be valuable to many practical applications in which a clean sEMG signal is a prerequisite for applying sEMG.

We have demonstrated that the proposed method adopts a better denoising procedure, which improves denoising result. We propose a denoising framework for sEMG signals based on CEEMD, component correlation analysis, and improved IT. The process removes noise from noisy data via correlation coefficients and improved IT. We use CEEMD to decompose an sEMG signal into several IMFs. By performing component correlation analysis and improved IT on the identified IMFs, the denoised sEMG signal is reconstructed using the modified and residual IMFs. To demonstrate the effectiveness of the proposed method, we have conducted numerical experiments with different SNR_{in} values for the sEMG signal derived from the standard database. The result confirms that the proposed method exhibits better performance in terms of stability and continuity compared with EMD, SWT, EMD-DT, and EMD-IT. Finally, the proposed method is applied to motion recognition. The results show that the recognition rate of the denoised sEMG is higher than that of the raw sEMG.

ACKNOWLEDGMENTS

This work was supported by the National Natural Science Foundation of China (Nos. 61671197, 61673350, and 60903084) and Zhejiang Public Welfare Technology Research (No. LGF18F010006).

REFERENCES

[1] R. H. Chowdhury *et al.*, "Surface electromyography signal processing and classification techniques," Sensors **13**(9), 12431–12466 (2013).
[2] J. E. Goh *et al.*, "Presentation-aid armband with IMU, EMG sensor and bluetooth for free-hand writing and hand gesture recognition," Int. J. Comput. Sci. Res. **1**(3), 65–77 (2018).
[3] M. Lyu *et al.*, "Design of a biologically inspired lower limb exoskeleton for human gait rehabilitation," Rev. Sci. Instrum. **87**(10), 104301 (2016).
[4] W. Chen *et al.*, "A cable-driven wrist robotic rehabilitator using a novel torque-field controller for human motion training," Rev. Sci. Instrum. **86**(6), 065109 (2015).
[5] M. Al Harrach *et al.*, "Denoising of HD-sEMG signals using canonical correlation analysis," Med. Biol. Eng. Comput. **55**(3), 375–388 (2017).
[6] K. Veer and V. Renu, "Analysis and recognition of operations using sEMG from upper arm muscles," Expert Syst. **34**(6), E12221 (2017).
[7] M. R. Mowla *et al.*, "Artifacts-matched blind source separation and wavelet transform for multichannel EEG denoising," Biomed. Signal Process. Control **22**(1), 111–118 (2015).
[8] R. K. Joseph, G. Titus, and M. S. Sudhakar, Biomed. Signal Process. Control **45**, 305–312 (2018).
[9] S. Mallat, *A Wavelet Tour of Signal Processing*, 2nd ed. (Academic Press, Orlanddo-SanDiego, 1999).
[10] A. O. Andrade, S. Nasuto, P. Kyberd, C. M. Sweeney-Reed, and F. R. van Kanijn, "EMG signal filtering based on empirical mode decomposition," Biomed. Signal Process. Control **1**(1), 44–55 (2006).
[11] V. Bajaj and A. Kumar, "Features based on intrinsic mode functions for classification of EMG signals," Int. J. Biomed. Eng. Technol. **18**(2), 156–167 (2015).
[12] K.-M. Chang and S.-H. Liu, "Gaussian noise filtering from ECG by Wiener filter and ensemble empirical mode decomposition," J. Signal Process. Syst. **64**(2), 249–264 (2011).
[13] K. M. Chang, "Arrhythmia ECG noise reduction by ensemble empirical mode decomposition," Sensors **10**(6), 6063–6080 (2010).
[14] X. Zhang and P. Zhou, "Filtering of surface EMG using ensemble empirical mode decomposition," Med. Eng. Phys. **35**(4), 537–542 (2013).
[15] M. Rakshit and S. Das, "An efficient ECG denoising methodology using empirical mode decomposition and adaptive switching mean filter," Biomed. Signal Process. Control **40**, 140–148 (2018).
[16] N. E. Huang, Z. Shen, S. R. Long, M. C. Wu, H. H. Shih, Q. Zheng, Y. C. Yen, C. C. Tung, and H. H. Liu, "The empirical mode decomposition and the Hilbert spectrum for nonlinear and non-stationary time series analysis," Proc. R. Soc. London **454**(1971), 903–995 (1998).
[17] Z. Wu and N. E. Huang, "Ensemble empirical mode decomposition: A noise assisted data analysis method," Adv. Adapt. Data. Anal. **1**(1), 1–14 (2009).
[18] J. R. Yeh, J. S. Shieh, and N. E. Huang, "Complementary ensemble empirical mode decomposition: A novel noise enhanced data analysis method," Adv. Adapt. Data. Anal. **2**(02), 135–156 (2010).

Published under license by AIP Publishing

[19]T. Guo and Z. Deng, "An improved EMD method based on the multi-objective optimization and its application to fault feature extraction of rolling bearing," Appl. Acoust. **127**, 46–62 (2017).
[20]Y. Kopsinis and S. Mclanglin, "Development of EMD-based denoising methods inspired by wavelet thresholding," IEEE Trans. Signal Process. **57**(4), 1351–1362 (2009).
[21]Y. Kopsinis and S. McLaughlin, "Empirical mode decomposition based denoising techniques," in 1st International Work-shop on Cognitive Information Processing (CIP), 2008.
[22]Y. Kopsinis and S. Mclanglin, "Empirical mode decomposition based soft thresholding," in Proceedings of the 16th European Signal Processing Conference, (EUSIPCO), Lausanne, Switzerland, 2008.
[23]H. Hao, H. L. Wang, and N. U. Rehman, "A joint framework for multivariate signal denoising using multivariate empirical mode decomposition," Signal Process. **135**, 263–273 (2017).
[24]G. Yang, Y. Liu, Y. Wang *et al.*, "EMD interval thresholding denoising based on similarity measure to select relevant modes," Signal Process. **109**, 95–109 (2015).
[25]J. Chen *et al.*, "An integrated method based on CEEMD-SampEn and the correlation analysis algorithm for the fault diagnosis of a gearbox under different working conditions," Mech. Syst. Signal Process. **113**, 102–111 (2018).
[26]S. Elouaham *et al.*, "Filtering of biomedical signals by using complete ensemble empirical mode decomposition with adaptive noise," Int. J. Comput. Appl. **149**(7), 39–43 (2016).
[27]Đ. T. Grozdić, S. T. Jovičić, and M. Subotić, "Whispered speech recognition using deep denoising autoencoder," Eng. Appl. Artif. Intell. **59**, 15–22 (2017).
[28]J. Srinivasan and V. Balasubramanian, "Low back pain and muscle fatigue due to road cycling—An sEMG study," J. Bodywork Mov. Ther. **11**(3), 260–266 (2007).
[29]J. Han and M. van der Baan, "Empirical mode decomposition for seismic time-frequency analysis," Geophysics **78**(2), O9–O19 (2013).
[30]J. Maier, A. Naber, and M. Ortiz-Catalan, "Improved prosthetic control based on myoelectric pattern recognition via wavelet-based de-noising," IEEE Trans. Neural Syst. Rehabil. Eng. **26**(2), 506–514 (2018).
[31]X. Xi *et al.*, "Evaluation of feature extraction and recognition for activity monitoring and fall detection based on wearable sEMG sensors," Sensors **17**(6), 1229 (2017).
[32]R. Rastogi, S. Sharma, and S. Chandra, "Robust parametric twin support vector machine for pattern classification," Neural Process. Lett. **47**(1), 293–323 (2018).

Published under license by AIP Publishing